

**SCHOOL OF MATERIALS AND MINERAL RESOURCES ENGINEERING
UNIVERSITI SAINS MALAYSIA**

**THE IMPACT OF DIFFERENT LATERAL SIZE OF GRAPHENE
OXIDE ON THE PERFORMANCE OF THE EMULSIFIED
ACRYLATE-BASED POUR POINT DEPRESSANT AND ITS
APPLICATION IN CRUDE OIL**

By

DARRYL WONG JUN CHEN

Supervisor: Prof. Azlan Ariffin

Dissertation submitted in fulfillment

of the requirements for the degree of Bachelor of Engineering with Honours

(Polymer Engineering)

Universiti Sains Malaysia

JUNE 2018

DECLARATION

I hereby declare that I have conducted, completed the research work and written the dissertation entitled **“The impact of different lateral size of graphene oxide on the performance of the emulsified acrylate-based pour point depressant and its application in crude oil”**. I also declare that it has not been previously submitted for the award of any degree or diploma or other similar title of this any other examining body or university.

Name of Student : Darryl Wong Jun Chen

Signature:

Date : 12th June 2018

Witness by

Supervisor : Prof. Azlan Ariffin

Signature:

Date : 12th June 2018

ACKNOWLEDGEMENTS

First and foremost, I would like to express the deepest appreciation to my supervisor, Prof. Azlan Ariffin for his continuous guidance and advice whenever I faced difficulties or problem in completing this dissertation. With his detailed review and constructive comment allowed me to complete this dissertation successfully.

Next, I would like to dedicate my appreciation to Mr Ridhwan, Phd student for his guidance, advices and suggestions throughout the duration of my research. His detail explanations regard technical and theoretical knowledge had eventually encouraged me and gave me more determination to complete my final year project.

I would also like to have special thanks to all laboratory assistants involved, especially Mr. Suharruddin and Mr. Zul for being a good technical support and whom always willing to offer help whenever I had encounter some technical problem during my research period.

Last but not least, I would like to send my sincere thanks to my family and friends for giving me tremendous moral support during the long preparation of thesis. Their support was invaluable and assists me to conquer any difficulties in completing my research project.

TABLE OF CONTENTS

Contents	Page
DECLARATION	ii
ACKNOWLEDGEMENTS	iii
TABLE OF CONTENTS	iv
LIST OF TABLES	ix
LIST OF FIGURES	xi
LIST OF ABBREVIATIONS	xvii
LIST OF SYMBOLS	xviii
ABSTRAK	xx
ABSTRACT	xxi
CHAPTER 1	1
INTRODUCTION	1
1.1 Research Background	1
1.2 Problem Statement	3
1.3 Research Objectives	4
1.4 Thesis Structure	4
CHAPTER 2	6
LITERATURE REVIEW	6
2.1 Crude Oil	6

2.1.1 Overview	6
2.1.2 Composition of Crude Oil	8
2.1.3 Rheology of Crude Oil	11
2.1.3.1 Newtonian and Non-Newtonian Model	11
2.1.3.2 Herschel-Buckley model	14
2.2 Introduction to Pour Point Depressant (PPD)	15
2.2.1 Overview	15
2.2.2 Common Type of PPD	16
2.2.3 Mechanism of Pour Point Depressant	19
2.2.4 Progression in PPD	24
2.2.4.1 PPD Solution	24
2.2.4.2 PPD Emulsion	25
2.2.4.3 PPD-Inorganic Material Composite	27
2.2.4.4 Factors Influence the Effectiveness of the PPD	29
2.3 Nano-hybrid Pour Point Depressant (NPPD)	30
2.3.1 Overview	30
2.3.2 Impact on Pour Point and Rheological Properties of Crude Oil	31
2.4 Introduction to Graphene Oxide (GO)	32
2.4.1 Overview	32
2.4.2 Properties of GO	33
2.4.3 Preparation of GO	35
2.4.4 Ultrasonication of GO	37
CHAPTER 3	42
METHODOLOGY	42
3.1 Materials	42

3.2 Experimental Method	42
3.2.1 Graphene oxide (GO)	42
3.2.1.1 Preparation of GO Samples	42
3.2.1.2 Characterisation of GO	44
3.2.1.2.1 Scanning Electron Microscopy (SEM)	44
3.2.1.2.2 Fourier Transform Infrared Spectroscopy (FTIR)	45
3.2.2 Emulsified Acrylate-Based PPD-GO	46
3.2.2.1 Preparation of Emulsified Acrylate-Based PPD-GO	46
3.2.2.2 Isothermal and Freeze thaw	48
3.2.2.3 Characterisation of Emulsified Acrylate-Based PPD-GO	49
3.2.2.3.1 Particle Size Distribution and Zeta Potential Measurement	49
3.2.2.3.2 Rheological Measurement	50
3.2.3 Application of Emulsified Acrylate-Based PPD-GO in Crude Oil	51
3.2.3.1 Pour Point Reduction for the Crude Oil	51
3.2.3.2 Rheological Measurement for Crude Oil doped with PPD-GO	53
CHAPTER 4	55
RESULTS AND DISCUSSIONS	55
4.1 Graphene Oxide	55
4.1.1 Morphology and Lateral Size Measurement of GO	55
4.1.2 Fourier Transform Infra-Red Spectroscopy (FTIR) Analysis	59
4.2 Emulsified Acrylate-based PPD-GO	61
4.2.1 Particle Size Distribution and Zeta Potential Measurement	61
4.2.1.1 The Addition of GO into Emulsified Acrylate-based PPD	61
4.2.1.2 The Addition of Different Lateral Size of GO into Emulsified Acrylate-Based PPD	65

4.2.1.3	Fresh and Aging Emulsified Acrylate-based PPD-GO at Isothermal	68
4.2.1.4	Particle Size Distribution and Zeta Potential for Fresh and Aging Emulsified Acrylate-based PPD-GO at Freeze Thaw	72
4.2.2	Rheological Measurement for Emulsified Acrylate-based PPD-GO	75
4.2.2.1	The Effect of Addition of GO on Rheological Behaviour of Emulsified Acrylate-Based PPD	75
4.2.2.2	The Effect Temperature on Rheological Behaviour of Emulsified Acrylate-Based PPD	78
4.2.2.3	The Effect of Different Lateral Size of GO on the Rheological Behaviour of Emulsified Acrylate-based PPD-GO	81
4.2.2.4	The Rheological Behaviour of the Fresh and Aging Emulsified Acrylate-Based PPD-GO with Different Lateral Size of GO	85
4.3	Application of Emulsified Acrylate-based PPD-GO into Crude Oil	90
4.3.1	Pour Point Reduction	90
4.3.1.1	Crude Oil Doped with Emulsified Acrylate-Based PPD-PPD-GO	90
4.3.1.2	Crude Oil Doped with Emulsified Acrylate-Based PPD-GO with Different Lateral Size of GO	92
4.3.2	Rheological Measurement for Crude Oil	93
4.3.2.1	Effect of Temperature on Rheological Behaviour of Crude Oil	93
4.3.2.2	The Rheological Behaviour of Crude Oil Doped Emulsified Acrylate- Based PPD and PPD-GO	98
4.3.2.3	The Rheological Behaviour of Crude Oil Doped Emulsified Acrylate- Based PPD-GO with Different Lateral Size of GO	101
CHAPTER 5		105
CONCLUSION AND RECOMMENDATIONS FOR FUTURE STUDIES		105

5.1 Conclusion	105
5.2 Recommendations for Future Works	106
REFERENCES	107

LIST OF TABLES

Table 4.1: Summary of FTIR spectrum	60
Table 4.2: Average particle size distribution and polydispersity index for EJV and EJGO 1	62
Table 4.3: Zeta potential for EJV and EJGO 1	64
Table 4.4: Average particle size distribution and polydispersity index for EJGO 1, EJGO 2, EJGO 3, EJGO 4 and EJGO 5	66
Table 4.5: Zeta potential for EJGO 1, EJGO 2, EJGO 3, EJGO 4 and EJGO 5	68
Table 4.6: Average particle size distribution and polydispersity index for fresh and aging EJGO 1, EJGO 2, EJGO 3, EJGO 4, and EJGO 5 at isothermal	70
Table 4.7: Zeta particle for fresh and aging EJGO 1, EJGO 2, EJGO 3, EJGO 4, and EJGO 5 at isothermal	71
Table 4.8: Average particle size distribution and polydispersity index for fresh and aging EJV, EJGO 1, EJGO 2, EJGO 3, EJGO 4 and EJGO 5 under freeze thaw	74
Table 4.9: Zeta potential for fresh and aging EJGO 1, EJGO 2, EJGO 3, EJGO 4, and EJGO 5 at freeze thaw	74
Table 4.10: Yield stress and power law index from Herschel-Buckley model for EJV and EJGO 1 at 30°C	76
Table 4.11: Yield stress and power law index from Herschel-Buckley model for EJGO 1, EJGO 2, EJGO 3, EJGO 4 and EJGO 5 at 30°C	82
Table 4.12: The yield stress and power law index from Herschel-Buckley model for fresh and aging EJV, EJGO 1, EJGO 2, EJGO 3, EJGO 4, EJGO 5 at 30°C	88

Table 4.13: Yield stress and power law index from Herschel-Buckley model of CO-Blank, CO-EJN and CO-EJGO 1 at 30°C 99

Table 4.14: Yield stress and power law index from Herschel-Buckley model of CO-EJGO 1, CO-EJGO 2, CO-EJGO 3, CO-EJGO 4, and CO-EJGO 5 at 30°C 103

LIST OF FIGURES

Figure 2.1: Wax deposition (Yang et al., 2015)	8
Figure 2.2: Percentage of composition in the crude oil (Dickneider T.A., 2004)	9
Figure 2.3: Thiophen derivatives (Eneh, 2011)	10
Figure 2.4: Carbazole (Eneh, 2011)	10
Figure 2.5: Phenol-type compound (Eneh, 2011)	11
Figure 2.7: Shear stress against shear rate for various fluid (Chhabra, 2010)	13
Figure 2.8: Molecular structure of the EVA copolymer (Li et al., 2017)	16
Figure 2.9: Chemical structure of comb-type copolymers: (a) MAC, (b) AMAC, and (c) NMAC (Xu et al., 2015)	19
Figure 2.10: PPD inhibition mechanism of wax modification. 2A) Chemical structure of wax 2B) Crystal shape of wax structure 2C) Crystal structure of growing wax lattice 2D) Polymeric additive with wax-like components 2E) Co-crystallization of wax and PPD 2F) sterically hindered wax structure (Wang et al., 1999)	20
Figure 2.11: The nucleation of the PPD (red) to the wax molecules (blue) (Hemant et al., 2008)	21
Figure 2.12: The adsorption and co-crystallisation of the PPD (red) to the wax molecules (blue) (Hemant et al., 2008)	22
Figure 2.13: Pictomicrographs of waxes a) crude oil without PPD and crude oil with PPD (Hemant et al., 2008)	23
Figure 2.14: The mechanism of interaction between comb-type copolymer with the paraffin wax molecules and the asphaltting in the crude oil (Li et al., 2017)	24
Figure 2.15: Emulsion types a) W/O b) O/W c) Multiple emulsion, W/OW (Hosyargar et al., 2012)	26

Figure 2.16: The mechanism interaction between NPPD with the paraffin wax molecules (Li et al., 2017)	28
Figure 2.17 : The PMMA-GO nano-hybrids mechanism (Al-Sabagh et al., 2016)	28
Figure 2.18: Lerf and Klinowski model of GO (Pei and Cheng, 2011)	35
Figure 2.19: Compressive stress and micro-jets on graphite oxide due to ultrasonication (Cai et al., 2017)	38
Figure 2.20: The lateral size of the with respect of ultrasonication time. (Kim et al., 2017)	39
Figure 2.21: GO synthesized through Hummers' method and undergo ultrasonication (Al-Sabagh et al., 2016).	41
Figure 3.1: Flowchart for preparation of GO samples	43
Figure 3.2: Flow chart for Scanning Electron Microscopy (SEM) of GO	44
Figure 3.3: Flowchart for Fourier Transform Infrared Spectroscopy (FTIR) of GO	45
Figure 3.4: Flowchart for preparation of emulsified acrylate-based PPD and PPD-GO	47
Figure 3.5: Flowchart for isothermal and freeze thaw of the emulsified acrylate-based PPD-GO	48
Figure 3.8 (a): Antoon Paar rheometer	51
Figure 3.8 (b): Spindle	51
Figure 3.9: Flowchart of pour point for the crude oil	52
Figure 3.10: Flowchart of rheological measurement for crude oil doped with PPD-GO	53
Figure 3.11: Flowchart on summary for methodology	54
Figure 4.1 (a): SEM images at 300 X magnification for GO 1	55
Figure 4.1 (b): SEM images at 300 X magnification for GO 2	55
Figure 4.1 (c): SEM images at 300 X magnification for GO 3	56
Figure 4.1 (d): SEM images at 300 X magnification for GO 4	56

Figure 4.1 (e) : SEM images at 300 X magnification for GO 5	56
Figure 4.2: Average lateral size of GO 1 (control), GO 2, GO 3, GO 4, and GO 5 against ultrasonication time.	58
Figure 4.3: Energy input on GO 1 (control), GO 2, GO 3, GO 4, and GO 5 with ultrasonication time.	58
Figure 4.4: FTIR spectrum	60
Figure 4.5: Particle size distribution curve for EJN and EJGO 1	62
Figure 4.6: The binding of the graphene derivatives on the surface of the interface of the oil droplets in O/W emulsion (Wu et al., 2017)	63
Figure 4.7: Particle size distribution curve for EJGO 1, EJGO 2, EJGO 3, EJGO 4 and EJGO 5	66
Figure 4.8 (a): Particle size distribution for fresh and aging EJGO 1 at isothermal	69
Figure 4.8 (b): Particle size distribution for fresh and aging EJGO 2 at isothermal	69
Figure 4.8 (c): Particle size distribution for fresh and aging EJGO 3 at isothermal	69
Figure 4.8 (d): Particle size distribution for fresh and aging EJGO 4 at isothermal	69
Figure 4.8 (e): Particle size distribution for fresh and aging EJGO 5 at isothermal	70
Figure 4.9 (a): Particle size distribution for fresh and aging EJGO 1 under freeze thaw	72
Figure 4.9 (b): Particle size distribution for fresh and aging EJGO 2 under freeze thaw	72
Figure 4.9 (c): Particle size distribution for fresh and aging EJGO 3 under freeze thaw	72
Figure 4.9 (d): Particle size distribution for fresh and aging EJGO 4 under freeze thaw	72
Figure 4.9 (e): Particle size distribution for fresh and aging EJGO 5 under freeze thaw	73
Figure 4.10: The shear stress against shear rate for EJN and EJGO 1 at 30°C	75
Figure 4.11: The viscosity against shear rate for EJN and EJGO 1 at 30°C	76
Figure 4.12: Separation distance between two acrylate-based droplets	77
Figure 4.13 (a): Shear stress against shear rate at 30°C	78

Figure 4.14 (a): Viscosity against shear rate at 30°C	78
Figure 4.13 (b): Shear stress against shear rate at 40°C	79
Figure 4.14 (b): Viscosity against shear rate at 40°C	79
Figure 4.13 (c): Shear stress against shear rate at 50°C	79
Figure 4.14 (c): Viscosity against shear rate at 50°C	79
Figure 4.13 (d): Shear stress against shear rate at 60°C	79
Figure 4.14 (d): Viscosity against shear rate at 60°C	79
Figure 4.15: The shear stress against the shear rate of EJGO 1, EJGO 2, EJGO 3, EJGO 4, and EJGO 5 at temperature 30°C	81
Figure 4.16: The viscosity against the shear rate of EJGO 1, EJGO 2, EJGO 3, EJGO 4 and EJGO 5 at temperature 30°C	82
Figure 4.17: The binding of different lateral size of GO nanosheets on the surface of the acrylate-based droplets interface	83
Figure 4.18: The binding of larger lateral size of GO (left) and binding of smaller lateral size of GO (right) on the acrylate-based droplets	84
Figure 4.17 (a): Shear stress against shear rate for fresh and aging EJN at 30°C	85
Figure 4.18 (a): Viscosity against shear rate for fresh and aging EJN at 30°C	85
Figure 4.17 (b): Shear stress against shear rate for fresh and aging EJGO 1 at 30°C	86
Figure 4.18 (b): Viscosity against shear rate for fresh and aging EJGO 1 at 30°C	86
Figure 4.17 (c): Shear stress against shear rate for fresh and aging EJGO 2 at 30°C	86
Figure 4.18 (c): Viscosity against shear rate for fresh and aging EJGO 2 at 30°C	86
Figure 4.17 (d): Shear stress against shear rate for fresh and aging EJGO 3 at 30°C	87
Figure 4.18 (d): Viscosity against shear rate for fresh and aging EJGO 3 at 30°C	87
Figure 4.17 (e): Shear stress against shear rate for fresh and aging EJGO 4 at 30°C	87
Figure 4.18 (e): Viscosity against shear rate for fresh and aging EJGO 4 at 30°C	87

Figure 4.17 (f): Shear stress against shear rate for fresh and aging EJGO 5 at 30°C	88
Figure 4.18 (f): Viscosity against shear rate for fresh and aging EJGO 5 at 30°C	88
Figure 4.19: The pour point reduction of CO-EJN and CO-EJGO 1	91
Figure 4.20: The pour point reduction of CO-EJGO 1, CO-EJGO 2, CO-EJGO 3, CO-EJGO 4 and CO-EJGO 5	92
Figure 4.21 (a): Shear stress against shear rate for CO-Blank, EJN, EJGO 1, EJGO 2, EJGO 3, EJGO 4, EJGO 5 at 30°C	94
Figure 4.22 (a): Viscosity against shear rate for CO-Blank, EJN, EJGO 1, EJGO 2, EJGO 3, EJGO 4, EJGO 5 at 30°C	94
Figure 4.21 (b): Shear stress against shear rate for CO-Blank, EJN, EJGO 1, EJGO 2, EJGO 3, EJGO 4, EJGO 5 at 40°C	94
Figure 4.22 (b): Viscosity against shear rate for CO-Blank, EJN, EJGO 1, EJGO 2, EJGO 3, EJGO 4, EJGO 5 at 40°C	94
Figure 4.21 (c): Shear stress against shear rate for CO-Blank, EJN, EJGO 1, EJGO 2, EJGO 3, EJGO 4, EJGO 5 at 50°C	95
Figure 4.22 (c): Viscosity against shear rate for CO-Blank, EJN, EJGO 1, EJGO 2, EJGO 3, EJGO 4, EJGO 5 at 50°C	95
Figure 4.23: Shear stress against shear rate for CO-Blank, CO-EJN and CO-EJGO 1 at 30°C	98
Figure 4.24: Viscosity against shear rate for CO-Blank, CO-EJN and CO-EJGO 1 at 30°C	99
Figure 4.25: The distance between paraffin chains increases when added with emulsified acrylate-based PPD-GO	100
Figure 4.26: Shear stress against shear rate for CO-EJGO 1, CO-EJGO 2, CO-EJGO 3, CO-EJGO 4, and CO-EJGO 5 at 30°C	102

Figure 4.27: Viscosity against shear rate for CO-EJGO 1 , CO-EJGO 2, CO-EJGO 3,
CO- EJGO 4, and CO-EJGO 5 at 30°C

102

LIST OF ABBREVIATIONS

PPD	Pour Point Depressant
GO	Graphene Oxide
PPD-GO	Pour Point Depressant-Graphene Oxide
NPPD	Nano-hybrid Pour Point Depressant
CO	Crude Oil
FTIR	Fourier Transform Infrared Analysis
SEM	Scanning Electron Microscopy
EJGO	Emulsified Acrylate-Based with Graphene Oxide
EJN	Emulsified Acrylate-Based without Graphene Oxide
DEA	Diethanolamine
DI	Deionised Water

LIST OF SYMBOLS

Hz	hertz
kHz	kilohertz
W	watt
g	gram
g^{-1}	per gram
s	second
s^{-1}	per second
J	joule
kg	kilometre
kPa	kilopascal
L	litre
mg	milligram
min	minute
mL	millilitre
mV	millivolt

Pa	pascal
Pa.s	pascal-econd
ppm	part per million
nm	nanometre
rpm	revolutions per minute
μm	micrometre
$^{\circ}\text{C}$	degrees Celsius
%	percent

**KESAN SAIZ SISI GRAFENA OKSIDA YANG BERBEZA TERHADAP
PRESTASI EMULSI BERASASKAN AKRILAT SEBAGAI PENGURANG
TITIK TUANG DAN APLIKASINYA DALAM MINYAK MENTAH**

ABSTRAK

Saiz sisi GO yang berbeza telah diperoleh melalui kaedah ultrasonikasi pada 0 min, 10 min, 30 min, 60 min dan 100 min. Keputusan SEM menunjukkan bahawa semakin lama masa ultrasonikasi, semakin kecil purata saiz helaian nano GO. FTIR digunakan untuk menunjuk kehadiran kumpulan berfungsi oksigen dalam helaian nano GO setelah tertakluk kepada ultrasonikasi. Penambahan GO yang mempunyai sisi berbeza ke dalam emulsi PPG-GO berasaskan akrilat menunjukkan saiz titisan berasaskan akrilat bertambah, lebih poli sebar dan mengurangkan keupayaan zeta. Walau bagaimanapun, apabila emulsi PPG-GO berasaskan akrilat berada dalam keadaan isothermal dan pembekuan cair, kesan saiz sisi GO yang berbeza selepas penuaan tidak begitu ketara. Pengukuran rheologi menunjukkan bahawa 10 minit adalah masa optimum ultrasonikasi untuk menghasilkan saiz helaian nano GO yang paling sesuai untuk meningkatkan aliran dan kestabilan emulsi PPG-GO berasaskan akrilat. Di samping itu, ia menunjukkan pengurangan paling banyak dalam titik tuang minyak mentah dan memulihkan rheologi minyak mentah dari segi tegasan ricih dan kelikatan. Melebihi masa optimum ultrasonikasi, pengurangan saiz sisi GO akan menghasilkan kesan negatif terhadap aliran dan kestabilan emulsi PPG-GO berasaskan akrilat dan prestasinya dalam minyak mentah. Akhir sekali, kajian mengenai model Herschel-Buckley telah terbukti lebih tepat dalam ramalan tekanan hasil dan tingkah laku bendalir emulsi PPG-GO berasaskan akrilat berbanding minyak mentah.

**THE IMPACT OF DIFFERENT LATERAL SIZE OF GRAPHENE
OXIDE ON PERFORMANCE OF THE EMULSIFIED ACRYLATE-
BASED POUR POINT DEPRESSANT AND ITS APPLICATION IN
CRUDE OIL**

ABSTRACT

The different lateral size of GOs were obtained through ultrasonication method at 0 min, 10 min, 30 min, 60 min and 100 min. The SEM results shows that the longer the ultrasonication time, the smaller the average lateral size of the GO nanosheets. The results from FTIR is used to shows the presence of the oxygen functional group in the GO nanosheets after subjected to ultrasonication. The addition of different lateral size GO into the emulsified acrylate-based PPD-GO shows that the acrylate-based droplets size increases, more polydisperse and reduce in zeta potential. However, when the emulsified acrylate PPD-GO is at isothermal and freeze thaw condition, the effect of the different lateral size of the GO after aging not that significant. The rheological measurement shows that 10 min is the optimum ultrasonication time to produce the ideal lateral size of GO nanosheets that leads to improvement in flowability and stability of the emulsified acrylate-based PPD-GO. Besides, it shows the highest reduction of pour point on the crude oil and improve rheological behaviour of the crude oil in terms of shear stress and viscosity. Exceeding the optimum ultrasonication time, the reducing lateral size of GO will produce negative impact on the flowability and the stability of the emulsified acrylate PPD-GO and its performance in crude oil. Lastly, the study on Herschel-Buckley model has proven to be more accurate in prediction of yield stress and fluid behaviour of emulsified acrylate-based PPD-GO compare to crude oil.

CHAPTER 1

INTRODUCTION

1.1 Research Background

The handling and transporting crude oil in petroleum industry through long distance pipelines from its source to the refinery has become a complex and highly technical operation (Manka et al., 2001). The transportation of crude oil via pipeline becoming more and more challenging because of the cold environment of the pipeline (Mehbad, 2017). The crude oil is a complex mixture of the hydrocarbons comprises waxes, resins, saturates asphaltenes, naphthanics and also dissolved gasses, water and salts (Ghotbi et al., 2016). From the composition of the crude oil, waxes which refers to the paraffin waxes has become the major challenge. This is because the precipitation of the paraffin waxes from the crude oil on the wall of the pipeline is causing serious problems at cold environment (Fang et al., 2012). This situation will adversely impact the pipeline operation such as decreased in production rates, increased power requirements and failure of facilities (Yang et al., 2015). Therefore, through many research and development over years scientist have come out with a brilliant solution whereby chemical treatment is used as an alternative to solve the problems. This chemical treatment is an additive added into the crude oil made from polymer known as pour point depressants (PPD).

PPD is a polymer additive that are added into crude oil to inhibit wax precipitation from the crude oil onto the wall of the pipeline and improve flow ability of crude oil at low temperature. PPD do not completely inhibit the precipitation of wax from crude oil, but just shift the precipitation toward a lower temperature (Chen et al., 2010). Generally, the mechanism for interaction between PPD with crude oil waxes

consists of nucleation, adsorption, co-crystallisation and solubilisation (Li et al., 2017). The effectiveness of the PPD can be measured by the ability of the PPD to withstand shear effect, temperature changing and aging of PPD. In short, the performance of PPD after mix with the crude oil is based on the shearing condition, thermal changes and stability of the PPD in crude oil (Yang et al., 2015). The commonly used types of PPD include ethylene-vinyl acetate (EVA) copolymers, comb polymers, and nano-hybrid (NPPD). Recently, the application of NPPD has drawn attention of many researchers. Therefore, to increase the performance of the PPD, the addition of nanoparticles is another alternative to enhance the performance of the PPD (Al-Sabagh et al., 2016).

The research on graphene oxide (GO) in improving the performance of the PPD is still limited. The performance of PPD-GO was studied by Al-Sabagh et al. (2016) has caught our attention. However, the study focuses on the loading of the GO. The study has shown PPD component has causes modification towards the size and the crystal shape of the wax molecule through co-crystallization of the polymer and paraffin chains. Whereas, the GO component consists of oxygen functional group which produces electrostatic repulsion between wax crystals. The study of the properties and the preparation of GO should be known before applying it into the PPD.

Recently, the used of ultrasonication method has enable different lateral size of GO to be obtained which in turns alter the properties of the GO. As mentioned by Kim et al. (2017) and Cai et al. (2017), the GO subjected to ultrasonication within a range of duration has causes the properties of the GO to be altered in terms degree of oxidation and of dispersion in the matrix of the polymer. Therefore, it is believes that the application of GO produced at different ultrasonication time in PPD may improve the quality of PPD in terms of thermal changes, shearing effect and storage stability. This

will eventually contribute to reduction of pour point and also rheological behaviour of the crude oil.

1.2 Problem Statement

The precipitation phenomenon adversely impacting the pipeline operation such as decreased in productions rates, increased power requirements and failure of facilities. This phenomenon reduces the effectiveness of the pipeline diameter and available area for the crude oil to flow which in turn causes a reduction in the pipe flow capacity and block the pipelines as times passes (Yang et al., 2015).

Emulsified acrylate-based PPD has been used to reduce precipitation of the waxes from the crude oil. However, the efficiency emulsified acrylate-based PPD alone in inhibiting the precipitation of waxes from the crude oil is still poor. Al-Sabagh et al. (2016) have concluded that the addition of nanomaterials which is GO into the PPD will shift the precipitation of the waxes from the crude oil to even lower temperature compares to that of PPD alone. At the same time improve the rheological behaviour of the crude oil. Therefore, addition of GO will improve the performance of emulsified acrylate-based PPD.

However, further studies on GO have shown that modified Hummers' method are producing stacked and large lateral size GO nanosheets. The dispersing efficiency were often limited by the size of two-dimensional GO which is large. This problem reduces the ability for GO to disperse in the emulsified acrylate-based PPD making it less efficient in inhibiting the precipitation of waxes from the crude oil. Kim et al. (2017) has proven that the ability to engineer the large size of GO can increase dispersability in the matrix of the composites.

Therefore, this investigation is to obtain the best lateral size via ultrasonication method which can increase the performance of emulsified acrylate-based PPD and its application in crude oil (Kim et al., 2017) (Cai et al., 2017). Ultrasonication may be one of the low-cost method to reduce the large size of GO rather than producing a smaller size GO through Hummer's method which is costly.

1.3 Research Objectives

This research is aim to develop different lateral size of graphene oxide (GO) via ultrasonication method which will impact on the emulsified acrylate-based pour point depressant (PPD) performance and its application in crude oil. To accomplish this main objective, this project was divided into three specific objectives:

- a) To prepare and study the different lateral size GO via ultrasonication method.
- b) To investigate the impact of different lateral size of the GO on the performance of emulsified acrylate-based PPD in terms of particles size distribution, zeta potential and rheological behaviour of the emulsified acrylate-based PPD-GO.
- c) To investigate the impact of emulsified acrylate-based PPD doped with different lateral size of GO on the pour point and rheological behaviour.

1.4 Thesis Structure

This thesis consists of 5 chapters.

Chapter 1 represents the introduction part of the thesis, which provides the background and problem statement of this research and an outline of the dissertation.

Chapter 2 contains literature review of thesis, which presents background literature on the information about crude oil, pour point depressant (PPD), nano-hybrid PPD (NPPD) and graphene oxide (GO). Crude oil is reviewed based on the challenge faces by

petroleum industry, composition and rheological behaviour of the crude oil in terms of non-Newtonian and Newtonian behaviour and Herschel-Buckley model. Besides, the PPD is reviewed based on common types of PPD, mechanism of PPD, PPD progression starts with PPD solution followed by PPD emulsion and PPD-inorganic materials composites and factors that influence the effectiveness of PPD. Next, focusing on the study of NPPD and its impact on the rheological behaviour of the crude oil. Finally, GO is reviewed based on its properties, preparation method and ultrasonication method of GO.

Chapter 3 represents the material approaches and research methodology of the project. This chapter will provide a detailed explanation regards the source of chemical and chemicals. The methodology consists of three parts. First, the methodology regarding the GO whereby the preparation of different lateral size of GO via ultrasonication method and characterisation method of GO will be discussed. Second, the methodology on preparation of emulsified acrylate-based PPD-GO and addition of different lateral size of GO into the PPD to produce emulsified acrylate-based PPD-GO. The characterisation of emulsified acrylate-based PPD-GO based on particle size distribution, zeta potential and rheological behaviour will be discussed. Lastly, on the application of emulsified acrylate-based PPD-GO with different lateral size of GO in crude oil, the methodology on pour point and rheological properties of the crude oil.

Chapter 4 shows the results discussion of the thesis. Elaboration on the problems and the explanation will be included in this chapter.

Chapter 5 denotes conclusion of the project. This chapter provide conclusion that based on the objectives of the projects and suggest recommendation for future studies.

CHAPTER 2

LITERATURE REVIEW

2.1 Crude Oil

2.1.1 Overview

Crude oil is found throughout the world. It have been produced for several decades in places like Egypt, China, India and North Sea (Yang et al., 2015). Crude oil is the most traded commodities in the world today. The fluctuating condition of the prices for the crude oil affect the supply and the demand. The demand on crude oil increases from day to day alongside with the development of the economy and society (Fang et al., 2012). For the past 20 years, the global demand for the crude oil has been increasing steadily. This can be proven as the global demand has grown by 24 million barrels per day from 60 million barrels per day to 84 million barrels per day. Report by the media showing that the market price of the heavy crude oil is lesser compare to the light crude oil (Ke-Jian and Guo-Min, 1997).

Today, in petroleum industry, handling and transporting crude oil through long distance pipelines from its source to the refinery has become a complex and highly technical operation (Manka et al., 2001). The cold environment around the pipelines has caused the transportation of crude oil via pipeline becoming more and more challenging (Mehbad, 2017). According to Marchesini et al., (2012) in the explored depths, the temperature of the sea floor is around 4°C.

Paraffin wax precipitation from crude oil is a serious problems during transportation and storage of crude oil (Ahmed et al., 2017) (He et al., 2016). This is because of the complex nature of the crude oil. The term used to describe the temperature at which the crude oil is still able to flow is called the pour point. Below the

pour point of the crude oil, there will be a complete absence of flow of the crude oil. Crude oil containing high amount of paraffin wax exhibit higher pour point (Deshmukh and Bharambe, 2008).

Paraffin wax from crude oil is a mixture of hydrocarbons consists of linear or normal chains which has carbon atoms ranging from 20 to 40 carbon atoms. The solubility of the higher-molecular waxes paraffin wax decreases as the temperature of the temperature reduce (Behbahani et al., 2015). The paraffin wax will actually precipitates from the crude oil at cold environment which has low temperature and deposited on the wall of the crude oil pipelines during the transportation of the crude oil to the refinery (Fang et al., 2012). The temperature gradient in the crude oil results in concentration gradient which creates a driving force. Driving force causes the movement of the paraffin wax from the crude oil toward the wall of the pipeline (Behbahani et al., 2015). According to Mehbad, (2017) , at low temperature the crystals of wax form an impermeable cakes. This results in blockage of the pipelines. Deshmukh and Bharambe, (2008) and He at al., (2016) also reported that the wax crystallization actually forms an interlocking network of the fine sheets and stated that the volume-spanning network is formed due to the presence of the attractive Van der Waals forces among the wax crystals. These fine sheets entrap the remaining liquid oil in cage-like structures which eventually results in the blockage of the pipeline because of the deterioration of the flow properties of the oil (He et al.,2016). The longer the time of the crude oil stays under low temperature, the larger the deposition of the paraffin wax on the crude oil on the inner wall of the pipelines as shown in Figure 2.1. This precipitation phenomenon reduces the effectiveness of the pipeline diameter and available area for the crude oil to flow which in turn causes a reduction in the pipe flow capacity and block the pipelines as times passes. This situation will adversely impacting the pipeline

operation such as decreased in productions rates, increased power requirements and failure of facilities (Yang et al., 2015).



Figure 2.1: Wax deposition (Yang et al., 2015)

The flow assurance has actually become the major technical and economic issue in crude oil transportation (Fang et al., 2012). The low crude's oil mobility and high viscosity is also one of major factor that pipeline transportation of crude oil is at high cost (Yaghi and Al-Bemani, 2002). Deposition of the paraffin wax will cause the reduction of the flow ability of the crude oil. Besides, during storage of the crude oil, paraffin wax deposition also might occur due to the crude oil temperature drop severely in the event of long production shutdown. This will lead to the occurrence of wax crystallization, followed by gelation and change in rheological behaviour of the crude oil (Marchesini et al., 2012). Therefore, storing of crude oil can also be difficult in winter or cold environment which reduce the fluidity due to deposition of wax fractions (Ke-Jian and Guo-Min, 1997).

2.1.2 Composition of Crude Oil

Crude oil is a fossil fuel. It is formed from heating and compression of plants and animals that died millions of years ago. Crude oil is smelly and mostly exists in yellow-to-black liquid (Eneh, 2011). Crude oil can be found in underground pools or reservoirs due to heat and pressure. Crude oil is removed from the underground pools or

reservoirs and it is separated through the refining process where different components of the crude oil will be separated (Demirbas and Bamufleh, 2017). The separation of the crude oil produces some useable petroleum products. These useable products include gasoline (petrol), kerosene, distillates such as diesel fuel and heating oil, jet fuel, lubricating oil petrochemical feed stock, paraffin wax and asphalt (Behbahani et al., 2015).

Generally, crude oil are complex chemical systems. Crude oil is consider as emulsion. This is because crude oil is a continuous hydrocarbon phase with drops of aqueous solution dispersed throughout the phase (A. Groysman, 2017). Crude oil are made up of hundreds of different hydrocarbon molecules (Demirbas and Bamufleh, 2017). The complex mixture of the hydrocarbons comprises waxes, resins, saturates, asphaltenes, naphthanics and also dissolved gasses, water and salts (Ghotbi et al.,2016). Dickneider T.A., (2004) shows that the percentage of composition in the crude oil with an API gravity of 35° is as shown in Figure 2.2.

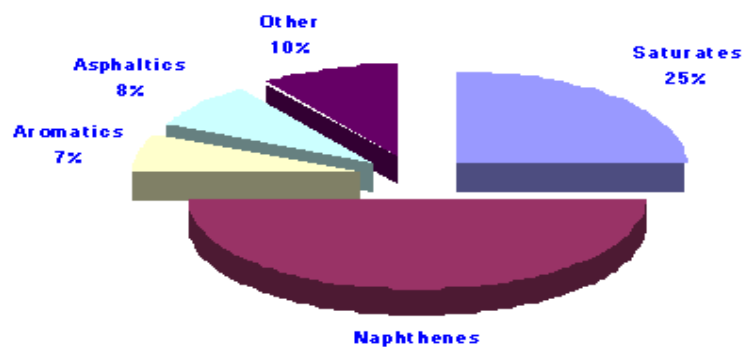


Figure 2.2: Percentage of composition in the crude oil (Dickneider T.A., 2004)

There are few of important compound that exist in the crude oil. One of them are the sulphur-containing compounds. The sulphur-containing compounds are thiol (mercaptans) like ethanethiol (C_2H_5SH). Besides, cyclic sulphides, such as the thiophen derivatives. Example of thiophen derivatives are tetrahydrothiophen and benzothiophen. Thiophen derivatives structures are as shown Figure 2.3.

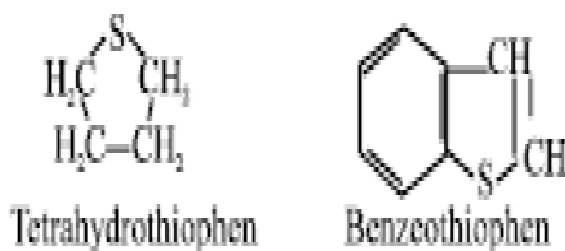


Figure 2.3: Thiophen derivatives (Eneh, 2011)

Nitrogen compounds can also be found in the crude oil and usually it is present in complex ring structures, such as carbazole as shown in Figure 2.4.

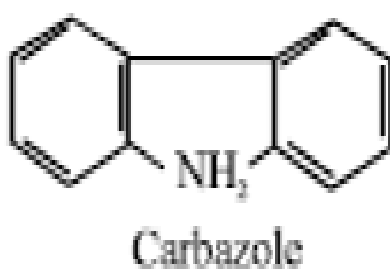


Figure 2.4: Carbazole (Eneh, 2011)

Crude oil also contains phenol-type compounds. This phenol-type compounds consist of hydroxyl group (-OH) attached to a benzene ring, such as phenol as shown in Figure 2.5.

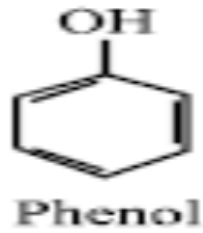


Figure 2.5: Phenol-type compound (Eneh, 2011)

Organic acids also present in crude oil. This organic acid are only small amounts in crude oil. Organic acids are molecules that have carbonyl group (-COOH). Example of the organic acids is the benzene carboxylic acid and its chemical structure are as shown in Figure 2.6.

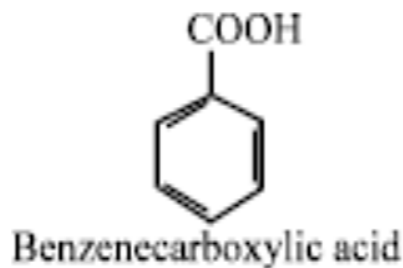


Figure 2.6: Organic acids (Eneh, 2011)

2.1.3 Rheology of Crude Oil

2.1.3.1 Newtonian and Non-Newtonian Model

The knowledge of fluid behaviour of the crude oil is crucial in petroleum industry in order for the proper design of piping and pumping of the crude oil. The different behaviour of the fluid may depend on the nature of the fluid. Fluids are characterized as Newtonian fluids or non- Newtonian fluids.

Newtonian fluids are described as the fluids with a simple linear relation between shear stress and shear rate. From the plot of shear stress against shear rate in Figure 2.7, the shear stress increase linearly with the shear rate whereby the gradient of the graph will determine the viscosity of the fluid. This shows that the viscosity remains constant although larger force exerts on the fluid to flow faster through a pipeline or channel. There are some examples of Newtonian fluids that we can relate with which include water, organic solvent and honey. Newtonian fluids obey the Newton law of viscosity, given by:

$$\tau = \eta \dot{\gamma} \quad \text{(Equation 2.1)}$$

where τ is the shear stress, Pa, $\dot{\gamma}$ is the shear rate, 1/s and η is apparent viscosity of the fluid, Pa.s (Omer, 2009).

Non-Newtonian fluids do not obey the Newton law of viscosity and are described as the fluids which displays a nonlinear relation between shear stress and shear rate. Non-Newtonian fluid consist of dilatant fluid and pseudoplastic fluid. The dilatant fluid is also known as the shear-thickening of the fluid whereas the pseudoplastic fluid is also known as the shear-thinning of the fluid. From the plot of shear stress against shear rate in Figure 2.7, the fluid shows dilatant fluid or shear thickening fluid behaviour when the shear stress of the fluid increases with the shear rate. The gradient from the shear thickening curve shows that the viscosity is increasing with shear rate. Whereas, pseudoplastic fluid or shear-thinning fluid behaviour from the plot shows shear stress of the fluid increases with shear rate. However, dilatant fluid shear stress increases more than pseudoplastic fluid with increasing shear rate. The

gradient of the shear thinning curve shows that the viscosity reduces with increasing shear rate. Non-Newtonian do not obey the Newton law of viscosity, given by:

$$\tau = k \dot{\gamma}^n \quad (2.2)$$

where τ is the shear stress, Pa, $\dot{\gamma}$ is the shear rate, 1/s, k is the consistency coefficient and n is the flow behaviour index. If the fluid showing a pseudoplastic or shear-thinning fluid behaviour, $n < 1$, Bingham plastic, $n=1$, dilatant fluid or shear thickening fluid behaviour, $n>1$ (Omer, 2009).

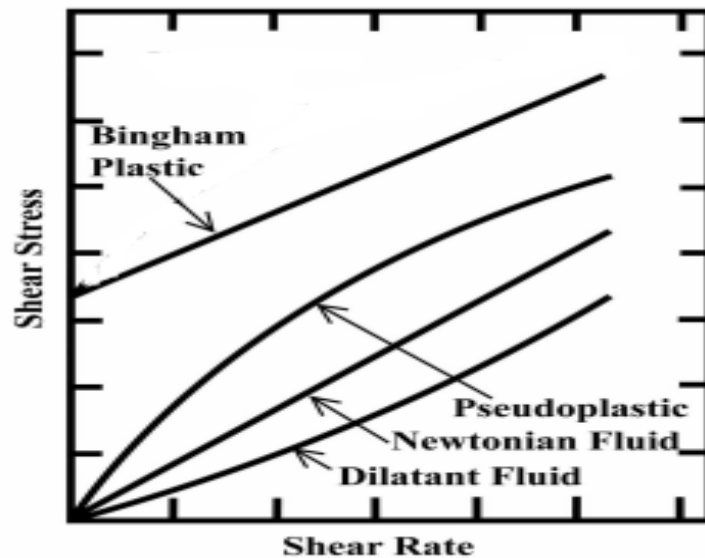


Figure 2.7: Shear stress against shear rate for various fluid (Chhabra, 2010)

The complex behaviour of crude oil leads to the research on rheological behaviour of crude oil. In the rheological studies of the crude oil, the knowledge on viscosity of crude oil is crucial. The rheology of the crude oil is affected by few factors.

As reported by Ariffina et al., (2016) the viscosities of the crude oil were strongly influenced by the shear rate, temperature and water contents or water volume fraction in the dispersed phase of the emulsion. The concentration of dispersed phase

has connection between the shear rate and viscosity whereby this behaviour is a result of droplets crowding. Besides, temperatures influence the viscosity of the crude oil emulsion through orientation of droplets, energy barrier and interfacial tension (Hosyargar et al., 2012). At high temperatures, the crude oils are simple Newtonian behaviour, the complexity increase below the crystallization temperature which the crude oil shows a non-Newtonian behaviour (Marchesini et al., 2012). The water contents or water volume fraction in the dispersed phase of the emulsion is greatly influenced by the hydrodynamic forces as well as the number of hydrogen bonds (Ariffina et al., 2016).

Therefore, crude oil will exhibit non-Newtonian behaviour when subjected to lower shear rate, lower temperatures and higher water volume fraction in the dispersed phase which will result in higher viscosity of the crude oil. This shear-thinning behaviour of the crude oil is more significant at these conditions. However, the crude oil will exhibit Newtonian behaviour at higher shear rate, higher temperature and lower water volume fraction in the dispersed phase. This means the viscosity is constant at increasing shear rate, temperature and decreasing water volume fraction in the dispersed phase in the crude oil emulsion (Ariffina et al., 2016).

2.1.3.2 Herschel-Buckley model

To understand Newtonian or non-Newtonian fluids behaviour, Herschel-Buckley model will be used to explain those behaviours. Taborda et al. (2017) mentioned Herschel-Buckley model to study the rheological behaviour of pseudoplastic substances. Tajnor et al. (2016) used Herschel-Buckley model, given by:

$$\tau = \tau_o + k \dot{\gamma}^n (\tau > \tau_o) \quad \text{(Equation 2.3)}$$

where τ is the shear stress, Pa, τ_o is the yield stress, Pa, k is the consistency factor, $\dot{\gamma}$ is the shear rate, 1/s, η is apparent viscosity of the fluid, Pa.s and n is the flow index to indicate the non-Newtonian shear-thinning behaviour of the crude oil (Tajnor et al., 2016) (Ariffina et al., 2016). From Herschel-Buckley model, the flow index, n indicates the flow behaviour of the fluid. When n less than 1, the fluid undergoes shear-thinning behaviour whereas n more than 1 the fluid undergo shear thickening behaviour. The yield stress, τ_o indicate the point whereby the fluid start to deformed under shear. The yield stress is either more than 0 or equal to 0 (Sochi and Blunt, 2008)

2.2 Introduction to Pour Point Depressant (PPD)

2.2.1 Overview

Pour point depressants (PPD) is a polymer additive that are added into crude oil to inhibit wax precipitation from the crude oil onto the wall of the pipeline and improve flow ability of crude oil at low temperature. PPD do not completely inhibit the precipitation of wax from crude oil, but just shift the precipitation toward a lower temperature (Chen et al., 2010). Besides, the commonly used types of PPD include ethylene-vinyl acetate (EVA) copolymers, comb polymers, and nano-hybrid PPD. Generally, the mechanism for interaction between PPD with crude oil waxes consists of nucleation, adsorption, co-crystallisation and solubilisation (Li et al., 2017). The effectiveness of the PPD can be related to the ability of the PPD to withstand shear effect, temperature changing and aging of PPD. In short, the performance of PPD after mix with the crude oil based on the shearing condition, thermal changes and stability of the PPD in crude oil (Yang et al., 2015). Therefore, to increase the performance of the PPD, the addition of nanoparticles is another alternative to enhance the performance of the PPD (Al-Sabagh et al., 2016).

2.2.2 Common Type of PPD

One of the earliest and most widely used polymeric PPDs are ethylene-vinyl acetate (EVA) copolymers. The molecular structure of the EVA is as shown in Figure 2.8. Based on the molecular structure, the crystalline phase acts as hydrophobic group is shown by the long segment of polyethylene chain of variable length. Whereas, the non-crystalline phase acts as the hydrophilic group is shown by the copolymerized vinyl acetate (VA) comonomer (Li et al., 2017).

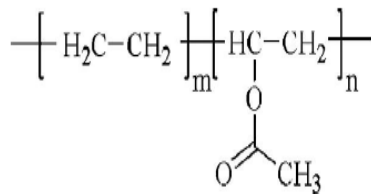


Figure 2.8: Molecular structure of the EVA copolymer (Li et al., 2017)

The application of EVA copolymer PPD can be found in some of the study to improve the performance of the EVA PPD in inhibiting the wax precipitation of the crude oil. Yang et al., (2017) studied the performance of EVA copolymer PPD through the addition of polymethylsilsesquioxane (PMSQ) microsphere. PMSQ microsphere alone is not efficient enough to improve the flow of the crude oil. Besides, by comparison, PMSQ microsphere is not as good compare to the traditional PPD. In the paper, the addition of PMSQ to the EVA copolymer PPD is said to improve the performance of EVA copolymer PPD towards the crude oil flow behaviour. This is because EVA molecules and PMSQ microsphere has form composite particles through the adsorption of EVA molecules on the PMSQ microsphere. This result in formation of nucleation templates for the precipitation of wax which form a larger wax microstructure and the further improving the flow behaviour of the oil. Therefore, the

right amount dosage of the PMSQ microsphere is crucial because it influence the amount of EVA copolymer PPD adsorbed by the microsphere (Yang et al., 2017).

Wu et al., (2008) studied the modification on EVA copolymer property through graft copolymerisation methods to improve its performance as PPD. Under controlled condition, the series of new EVA graft copolymer with new side chains. The graft component used is the maleic anhydride and high carbonic amine, BPO as initiator, toluene as solvent. The new graft EVA copolymer performance in the enhancement of flow behaviour of crude oil is better compare to EVA copolymer (Wu et al., 2008).

Anisuzzaman et al., (2017) studied the performance of EVA as control sample, ethylene vinyl acetate co-methyl methacrylate (EVA co-MMA) and ethylene vinyl acetate co-diethanolamine (EVA co-DEA) on the crude oil. Addition of MMA and DEA is said to improve the performance of EVA. The results have shown that the EVA co-DEA is better than EVA and EVA co-MMA in terms of pour point and cloud point. Whereas EVA and EVA co-MMA has shown a similar results of pour point and cloud point. Therefore, EVA co-MMA has shown the highest percentage of reduction of wax precipitation in crude oil (Anisuzzaman et al., 2017) .

Fang et al. (2012) has prepared a new-style of PPD by mixing the aminated copolymer and EVA copolymer in fixed proportion. The aminated copolymer was produce through the amination of terpolymer copolymerized with monomers maleic anhydride, octadecyl acrylate and vinyl acetate. The results obtained from the FTIR , differential scanning calorimetry (DSC), and cross-polarized light microscopy has showed that the new PPD could forms agglomerates which has become the efficient nucleator of the crude oil. This studies has changed the wax crystallization process and reduce the pour point of the crude oil (Fang et al., 2012).

In recent years, comb-type copolymers have become more abundant and more research has been done to apply comb copolymer in reducing the pour point of the crude oil. Figure 2.9 shows some of the example of the chemical structure of comb-type maleic anhydride- α -octadecene copolymer and its derivatives with octadecyl (MAC), phenyl (AMAC), or naphthalene (NMAC) pendants. Unlike EVA, the comb-type copolymer consists of polyethylene in the side pendant alkyl chains. The molecular structure of a comb type copolymers consists of long chain alkyl groups which is hydrophobic and nonpolar. Whereas, the polar group will be the aromatic base, ester bond, amine bond and etc.

Xu et al. (2015) investigated the role pendant group in the comb-type copolymers influencing the flow behaviour of the crude oil. The maleic anhydride- α -octadecene copolymer and its derivatives with octadecyl (MAC), phenyl (AMAC), or naphthalene (NMAC) pendants were synthesized and their chemical structure are as shown in the Figure 2.8. The addition of these derivatives to the crude oil has alter the size and the quantity of the paraffin crystals. Besides, the flow ability in terms of viscosity and yield stress of the crude oil has improved. These derivatives have successfully reduced the paraffin crystallization temperature and the also the quantity of the wax precipitation. The results show that AMAC is the best in improving the flow of the crude oils because it has small aromatic pendants that adsorb on the surface of the asphaltenes in the crude oil. However, NMAC does not show the best in improving the flow of the crude oils compare to MAC and AMAC because of the presence of the large aromatic pendants which produce higher stearic hindrance that impair the assembly of the copolymer with asphaltenes (Xu et al., 2015).

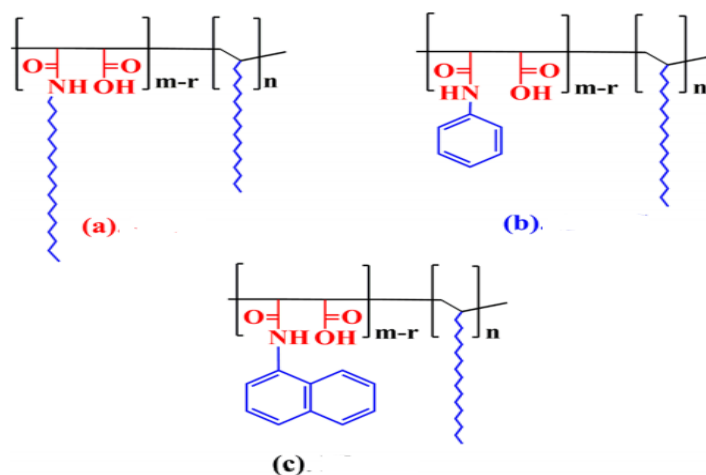


Figure 2.9: Chemical structure of comb-type copolymers: (a) MAC, (b) AMAC, and (c) NMAC (Xu et al., 2015)

Based on the studies by Li et al., the model oil flowability can be improved through the assembly of comb-type copolymers with paraffin and asphaltene. The studies has found out that the used of comb-type (maleic acid alkylamides-co- α -octadecene) copolymers (MACs) are more effective compare to poly(ethylene-butene) copolymers in improving the flow ability of crude oils containing alphaltnenes. MACs are said to alter the size and the shape of the paraffin wax crystals upon cooling. Besides, upon cooling the stabilization of the crude oil by the stearic effects of the long alkyl chains of MAC which reduces the strength of paraffin or asphaltene gels is contributed by the interaction between the amide groups and carboxyl of MAC with the aromatic groups of alphaltenes. Therefore, comb-type copolymers has appear to be significantly reduce the precipitation of wax (Li et al., 2012).

2.2.3 Mechanism of Pour Point Depressant

Generally, the mechanism for interaction between PPD with crude oil waxes are through nucleation, adsorption, co-crystallisation and solubilisation (Li et al., 2017). These are the prevention or inhibition mechanism of interlocking wax crystals by PPD

(Hemant et al., 2008) (Wang et al., 1999). These mechanisms have caused the modification towards the morphology of the crystal in the crude oil, the reduction of the motion order of the wax molecules and reduction of interacting force between wax molecules. Through the addition of PPD into the crude oil, the tendency for the wax crystal to interlock and form a three-dimensional network has decreased (Yang et al., 2015). Figure 2.10 has shown clearly and briefly of the PPD inhibition mechanism of wax modification.

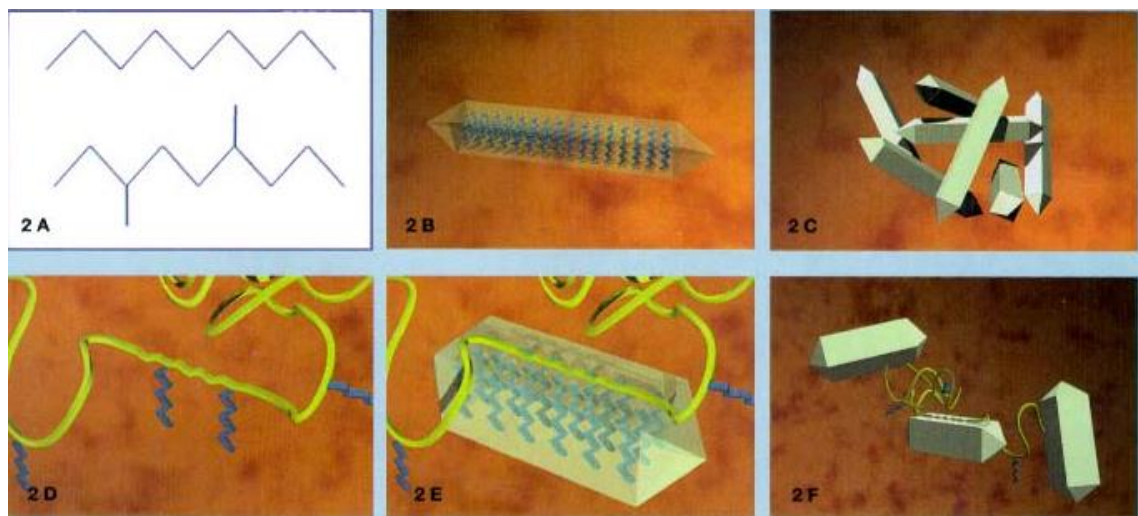


Figure 2.10: PPD inhibition mechanism of wax modification. 2A) Chemical structure of wax 2B) Crystal shape of wax structure 2C) Crystal structure of growing wax lattice 2D) Polymeric additive with wax-like components 2E) Co-crystallization of wax and PPD 2F) sterically hindered wax structure (Wang et al., 1999)

According to Yang et al. (2015) and Li et al. (2017), in nucleation mechanism when the temperature falls below the temperature at which the crude oil first precipitates which is called the wax appearance temperature (WAT), the attraction between the wax molecules is greater than that between wax and crude oil. The larger attraction forces between the wax molecules has caused the wax molecules to be precipitated from the oil phase. The wax molecules act as crystalline nucleus initiate the formation of the wax crystal which will be precipitated on the pipeline. Whereas for the

PPDs molecules will undergo precipitation at this nucleation stage as shown in Figure 2.11. The PPDs molecules forms aggregates and undergo polynucleation whereby the sub-critical crystalline nucleus is formed. This sub-critical nucleus formation has led to prevention of wax crystal growth and also promotes smaller wax crystals (Yang et al., 2015) (Li et al., 2017).

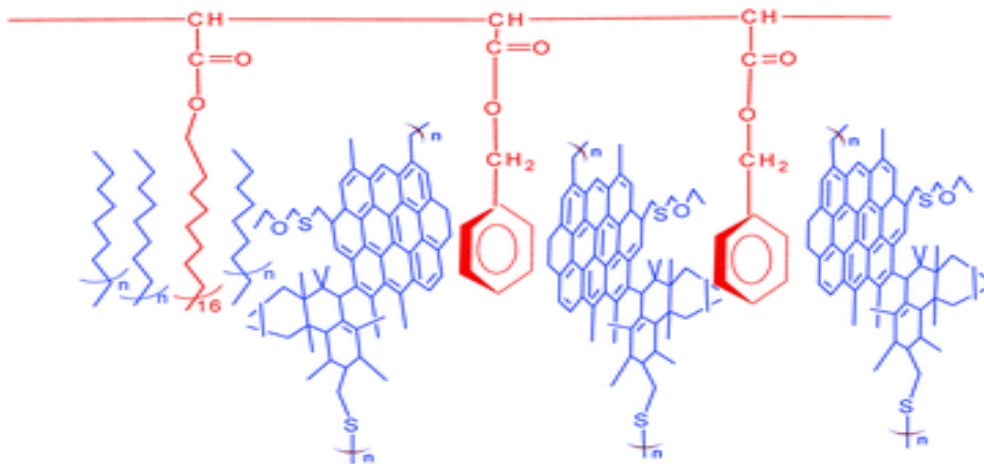


Figure 2.11: The nucleation of the PPD (red) to the wax molecules (blue) (Hemant et al., 2008)

According to Hermant et al., (2008), the Figure 2.12 shows that adsorption and co-crystallisation of the PPD towards the wax molecules and the and polar component of the PPD (green) which hinder co-crystallisation of wax molecules (Hermant et al., 2008). Co-crystallisation occurs below WAT where adsorption of the wax molecules towards the surfaces of the PPDs occur. In the process of wax precipitation, the wax molecules are coated with solvent components. The PPDs alter the morphology of wax crystals formed from long stick-like or plate-like structure to small spherical-like in crude oil. Again, addition of PPDs has caused disruption to the growth of the wax

crystals, inhibits wax precipitation and also improves rheological behaviour of the crude oil (Yang et al., 2015) (Li et al., 2017).

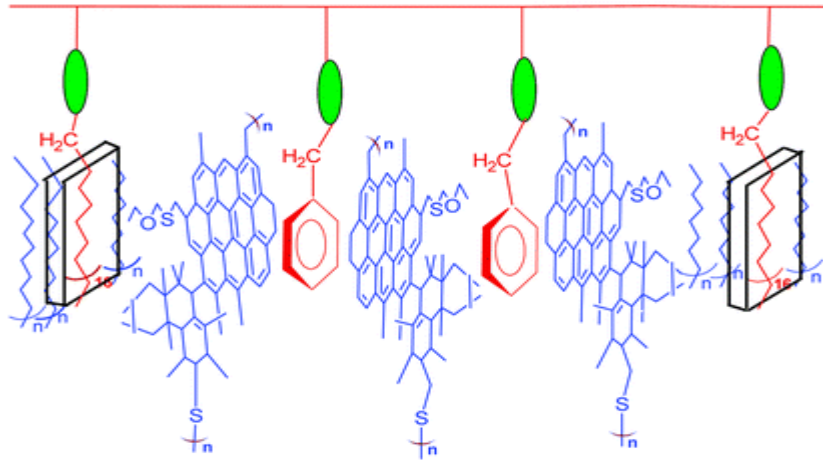


Figure 2.12: The adsorption and co-crystallisation of the PPD (red) to the wax molecules (blue) (Hemant et al., 2008)

In solubilisation mechanism, the addition of PPDs into the crude oil has causes high dispersion of small wax crystals as shown in Figure 2.13 (Hemant et al., 2008). The polar groups can be found on the surface of the eutectic formed by the PPDs molecules and wax crystal. The formation of the first molecular layer is through the adsorption of the low molecular polarity substances in crude oil with the polar groups on the eutectic surface. Then, the solvation layer is the outmost surface of the eutectic which is also the secondary layer is induced by the adjacent first layer. The wax crystal-liquid interface nature changed due to the presence of the solvation layer which at the same time leading to the reduction of the surface energy in the system. The connection between the wax crystals is prevented same goes to the formation of three-dimensional network structure by the solvation layer (Yang et al., 2015) (Li et al., 2017).

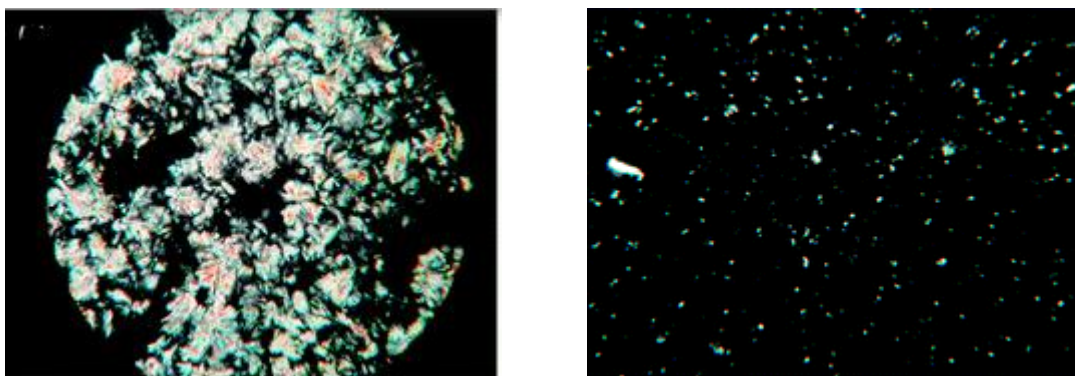


Figure 2.13: Pictomicrographs of waxes a) crude oil without PPD and crude oil with PPD (Hemant et al., 2008)

However, different types of PPD has their own way of inhibiting the wax crystal from growing. The effectiveness of the mechanism of interaction between the EVA copolymer is dependent on the VA content. At low VA contents, the EVA copolymer have higher crystallinity and acts nucleating agents. Whereas, at higher VA contents the ability of the crystallization for the EVA copolymers interact with the paraffin wax becomes weaker. Due to the weakness of the EVA copolymer, EVA structure is sometimes incorporated with surface-active groups to dispersed and inhibit the growth of the wax crystals (Yang et al., 2015) (Li et al., 2017).

For the comb-type copolymer as shown in Figure 2.14, the mechanism of interaction is between the comb-type copolymer with the paraffin crystal and the asphaltene in the crude oil. Co-crystallization causes the long chain paraffin crystals anchored the non-polar alkyl branches of the comb-type copolymer. Besides, the asphaltene in the crude oil is surrounded by the polar groups of the comb-type copolymer. The comb-type copolymer can cause the asphaltenes to be decentralized and inhibit the formation of the network structure (Yang et al., 2015) (Li et al., 2017).

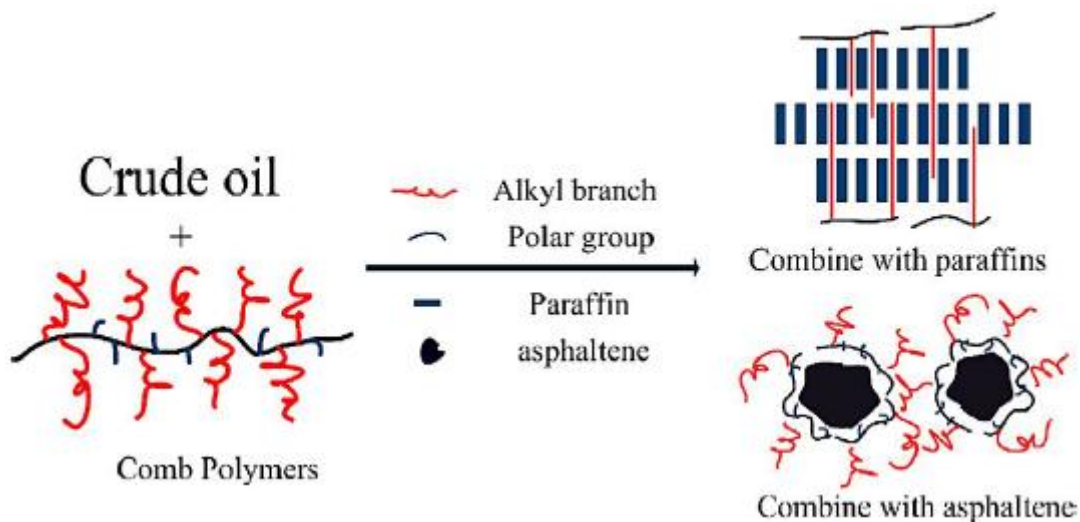


Figure 2.14: The mechanism of interaction between comb-type copolymer with the paraffin wax molecules and the asphaltene in the crude oil (Li et al., 2017)

2.2.4 Progression in PPD

2.2.4.1 PPD Solution

PPD solution is a traditional type PPD which has a number average of molecular weight of at least 500. It is the earliest polymer additive or chemical treatment method that is commonly used in petroleum industry to inhibit the wax precipitation phenomenon in crude oil.

PPD solution has high melting point. The high melting properties cause the PPD solution tend to solidified and insoluble at room temperature. The tendency of PPD solution to solidify easily making it even harder if it is utilised in a cold climate country like Europe or Australia. Regardless of which country PPD solution is utilised, the PPD solution needs to be heated at high temperature around 45°C to 50°C (A. Admiral et al., 2016).

Heating is required to turn the solidified PPD solution at room temperature to a soluble solution before it can be applied in crude oil to inhibit wax precipitation phenomenon. This shows that application of the PPD solution into the crude oil without